

Available online at [www.sciencedirect.com](http://www.sciencedirect.com)
**jmr&t**  
 Journal of Materials Research and Technology
[www.jmrt.com.br](http://www.jmrt.com.br)

## Original Article

# Characterization of plasma nitrided layers produced on sintered iron

 Marcos Alves Fontes<sup>a</sup>, Ricardo Gomes Pereira<sup>b</sup>, Frederico Augusto Pires Fernandes<sup>b</sup>,  
 Luiz Carlos Casteletti<sup>b</sup>, Pedro Augusto de Paula Nascente<sup>a,\*</sup>
<sup>a</sup> Departamento de Engenharia de Materiais, Universidade Federal de São Carlos, São Carlos, SP, Brazil<sup>b</sup> Departamento de Engenharia de Materiais, Universidade de São Paulo, Escola de Engenharia de São Carlos, São Carlos, SP, Brazil

## ARTICLE INFO

## Article history:

Received 16 October 2013

Accepted 16 April 2014

Available online 7 June 2014

## Keywords:

Plasma nitriding

Powder sintered metal

Scanning electron microscopy

X-ray diffraction

## ABSTRACT

Plasma nitriding is a thermo-physical-chemical treatment process, which promotes surface hardening, caused by interstitial diffusion of atomic nitrogen into metallic alloys. In this work, this process was employed in the surface modification of a sintered ferrous alloy. Scanning electron microscopy (SEM), X-ray diffraction (XRD) analyses, and wear and microhardness tests were performed on the samples submitted to ferrox treatment and plasma nitriding carried out under different conditions of time and temperature. The results showed that the nitride layer thickness is higher for all nitrided samples than for ferrox treated samples, and this layer thickness increases with nitriding time and temperature, and temperature is a more significant variable. The XRD analysis showed that the nitrided layer, for all samples, near the surface consists in a mixture of  $\gamma'$ -Fe<sub>4</sub>N and  $\epsilon$ -Fe<sub>3</sub>N phases. Both wear resistance and microhardness increase with nitriding time and temperature, and temperature influences both the characteristics the most.

© 2014 Brazilian Metallurgical, Materials and Mining Association. Published by Elsevier Editora Ltda. Este é um artigo Open Access sob a licença de CC BY-NC-ND

## 1. Introduction

Many thermal treatments have been used to improve the mechanical properties of material surfaces, such as hardness and wear resistances. Nitriding is a commonly used surface treatment for obtaining these improvements due to the facility in its use, relatively low cost, and good ability to improve surface hardness and resistance to wear and corrosion [1]. Among

the three different types of nitriding processes, liquid, gas, and plasma (or ion), the latter can be considered the best one because it presents positive characteristics such as a precise control of the surface layers, low energy and gas consumptions, not generating environmental pollution and allowing thermal treatments at low temperatures (below 500 °C) [1].

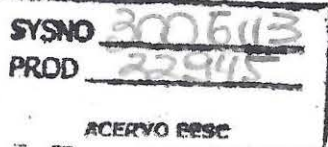
Ion nitriding is a thermal-physical-chemical treatment process that provokes surface hardening by interstitial diffusion of atomic nitrogen into both ferrous and non-ferrous metallic

\* Corresponding author.

E-mail: [nascente@ufscar.br](mailto:nascente@ufscar.br) (P.A.P. Nascente).<http://dx.doi.org/10.1016/j.jmrt.2014.04.003>

2238-7854/© 2014 Brazilian Metallurgical, Materials and Mining Association. Published by Elsevier Editora Ltda.

Este é um artigo Open Access sob a licença de CC BY-NC-ND



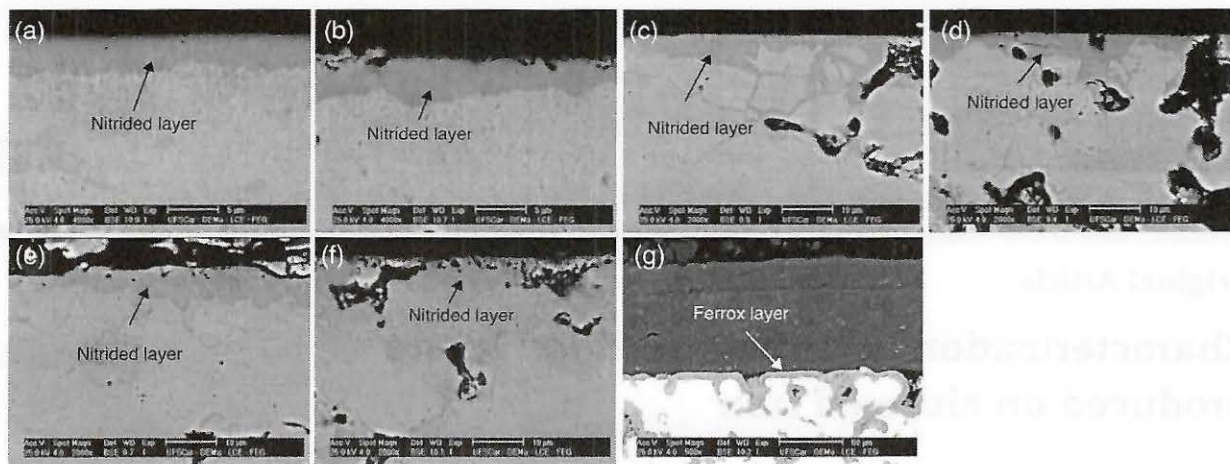


Fig. 1 – SEM micrographs of the plasma nitrided samples, and sample submitted to the ferrox treatment.

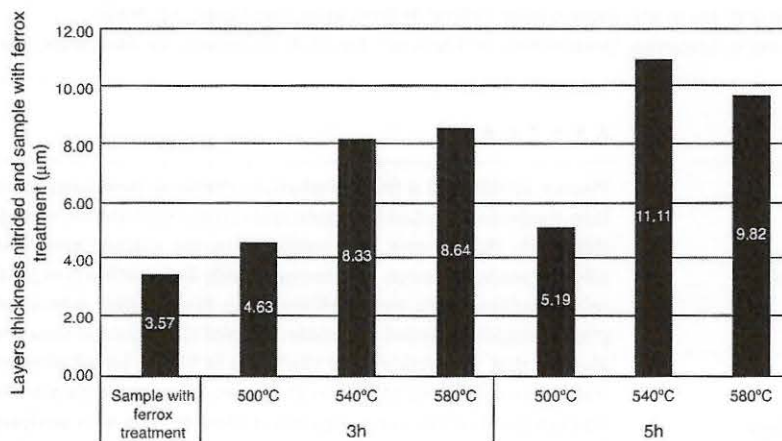


Fig. 2 – Thickness values for the plasma nitrided samples, untreated sample, and sample submitted to the ferrox treatment.

surfaces [2]. This process causes the formation of a case layer, which may comprise an oxide layer, a compound layer, and a diffusion zone [3,4]. In the case of ferrous alloys, the compound layer, also called white layer, is constituted of mainly  $\gamma'$ -Fe<sub>4</sub>N,

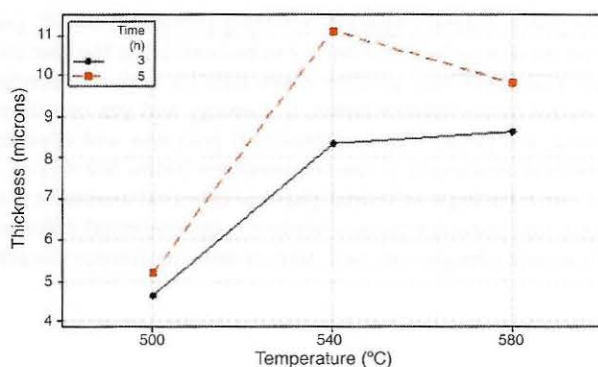


Fig. 3 – Thickness as a function of the nitriding parameters (temperature and time).

$\epsilon$ -Fe<sub>3</sub>N, and possibly Fe<sub>2</sub>N [5–10]. The diffusion zone (or diffusion layer) is formed between the compound layer and the matrix, and consists of nitrides formed with not only iron but also high affinity metals such as aluminum, chromium, vanadium, and molybdenum [11]. It is very important to control the nitriding parameters in order to obtain the best performance of nitrided components used in different engineering applications [11]. The composition and thickness of the nitrided layers are directly related to the treatment temperature, pressure, and time, as well as the composition of the base material [12–14].

Table 1 – Chemical composition (wt.%) of the sintered iron sample.

Element	wt. %
Carbon combined	0.20–0.40
Copper	1.75–2.25
Sulfur	0.14–0.22
Iron	Remainder



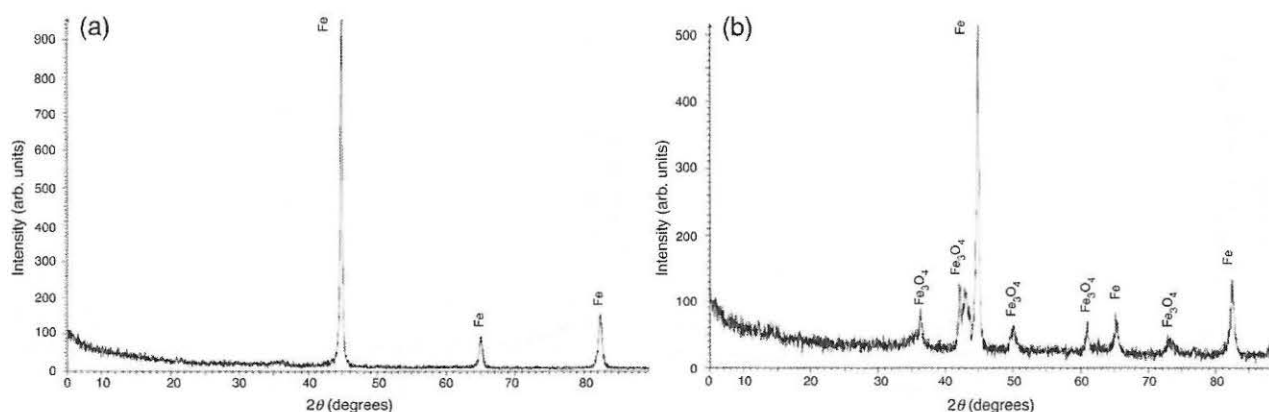


Fig. 4 – XRD diffractograms for the untreated and ferrox treated sintered ferrous alloy samples.

The objective of this work was to characterize the nitrided layers formed on iron sintered samples with and without ferrox treatment. Different nitriding times (3 and 5 h) and temperatures (500, 540, and 580 °C) were employed and the characterization was performed by scanning electron microscopy (SEM), X-ray diffraction (XRD) analyses, and wear and microhardness tests.

## 2. Methods

Table 1 shows the nominal chemical composition of the samples used in this work. These samples had one of their faces progressively grinded on 220, 320, 400, 500, 600, and 900 meshes, polished on 0.05 μm alumina abrasive, washed in water and alcohol, dried, and stored. Right before being placed into the nitriding reactor, the samples were ultrasonically washed with tetrachlorethylene for 60 min in order to remove grease and impurities from the surface.

A cleaning treatment by argon sputtering for one hour was performed inside the reactor chamber before the plasma nitriding treatment. The plasma nitriding conditions were as follows: a gas mixture of 80 vol.% H<sub>2</sub> and 20 vol.% N<sub>2</sub>; a pressure

of 5 mbar; temperatures of 500, 540, and 580 °C; and periods of 3 and 5 h.

The microstructural analysis was carried out using a Philips SL-30 field emission gun (FEG) scanning electron microscope equipped with an energy-dispersive spectrometer (EDS). The samples were coated with gold and silver to allow electrical contact to the sample holder. The images were acquired by employing the backscattering electron (BSE) method.

X-ray diffraction (XRD) characterization was performed using a Rigaku Geiger-Flex equipment under the following conditions: Cu Kα radiation ( $\lambda = 1.54056 \text{ \AA}$ ),  $2\theta$  step scan of  $0.032^\circ$  per second, in the range of  $5-90^\circ$ . Spectral evaluation was done using the Diffrac EVA (release 2001) software.

The wear tests were carried out in a fixed ball device using a 52100 steel sphere of 25.4 mm diameter, a rotation speed of 300 rpm, a load of 245 g (2.45 N), and testing times of 5, 10, 20, and 30 min [15]. The removed volume ( $V$ ) of each crater was evaluated according to the following equation [16]:

$$V = \pi \frac{b^4}{64 \cdot R^2} \left( R - \frac{b^2}{8 \cdot R} \right) \approx \frac{\pi b^4}{64 \cdot R} \quad b \ll R, \quad (1)$$

where  $b$  is the cap diameter and  $R$  is the sphere radius.

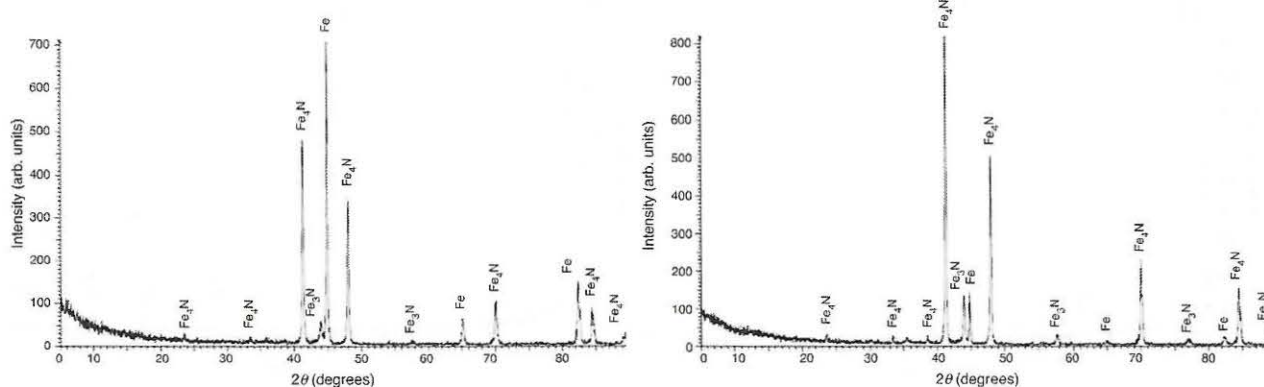


Fig. 5 – XRD diffractograms for plasma nitriding temperature of 500 °C.

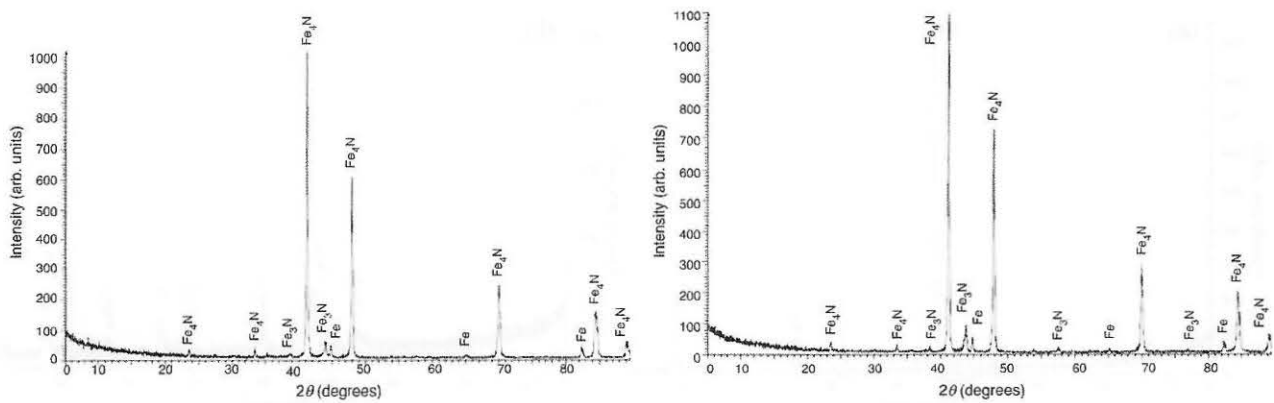


Fig. 6 – XRD diffractograms for plasma nitriding temperature of 540 °C.

The microhardness measurements were obtained using a Buehler hardness tester, in a Vickers scale (HV), with a load of 100 gf. For each specimen, eight measurements were done at as many different points on the surface.

### 3. Results and discussion

#### 3.1. SEM analysis

Fig. 1 depicts the SEM micrographs of the ferrous alloy samples plasma nitrided at 500 °C for (a) 3 and (b) 5 h; at 540 °C for (c) 3 and (d) 5 h; at 580 °C for (e) 3 and (f) 5 h; and (g) the ferrous alloy sample subjected to a ferrox treatment. It can be observed that the greater diffusion of nitrogen was seen for the samples treated at both 540 and 580 °C. The thicknesses of the modified layers are presented in Fig. 2.

Higher thickness values were presented by the samples treated for 5 h in comparison with those treated for 3 h, for a given treatment temperature, as shown in Fig. 3. For sintered parts where the porosity is predominantly open, the layer thickness, at a given temperature, may increase with the nitriding time [17].

It can be observed from Fig. 3 that the temperature variable predominates over the time variable for sintered ferrous alloy samples subjected to plasma nitriding treatment. The non-steady state diffusion theory (Fick's second law) could be used to explain the results, by using the expression  $x = \sqrt{Dt}$ , that is, the nitride layer thickness is less dependent on  $t$  – time (non-linearly) than on  $T$  – temperature (exponentially). Thus, increasing the nitriding time is not the most favorable way to obtain thicker layers for this material.

#### 3.2. XRD analysis

Fig. 4 displays the XRD diffractograms for the sintered ferrous alloy sample (a) without any treatment and (b) with the ferrox treatment. For the non-treated sintered ferrous alloy sample, the diffraction peaks shown in Fig. 4(a), with  $2\theta$  at 44.6, 65, and 82.3°, corresponding to (110), (200), and (211) diffraction planes, respectively, are associated to polycrystalline  $\alpha$ -Fe (ferrite). After the ferrox treatment, not only Fe but also  $\text{Fe}_3\text{O}_4$  peaks were identified.

Figs. 5–7 display the XRD diffractograms for the samples nitrided at 500 °C (Fig. 5), 540 °C (Fig. 6), and 580 °C (Fig. 7) for (a) 3 and (b) 5 h, revealing the presence of  $\gamma$ - $\text{Fe}_4\text{N}$  and, in a lesser scale,  $\epsilon$ - $\text{Fe}_3\text{N}$  phases. The  $\alpha$ -Fe peaks appear due to the

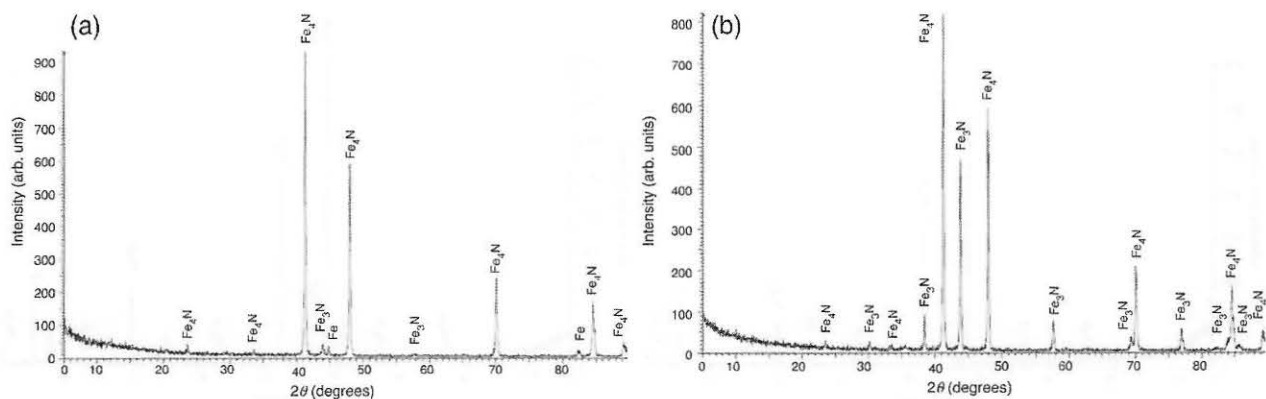


Fig. 7 – XRD diffractograms for plasma nitriding temperature of 580 °C.



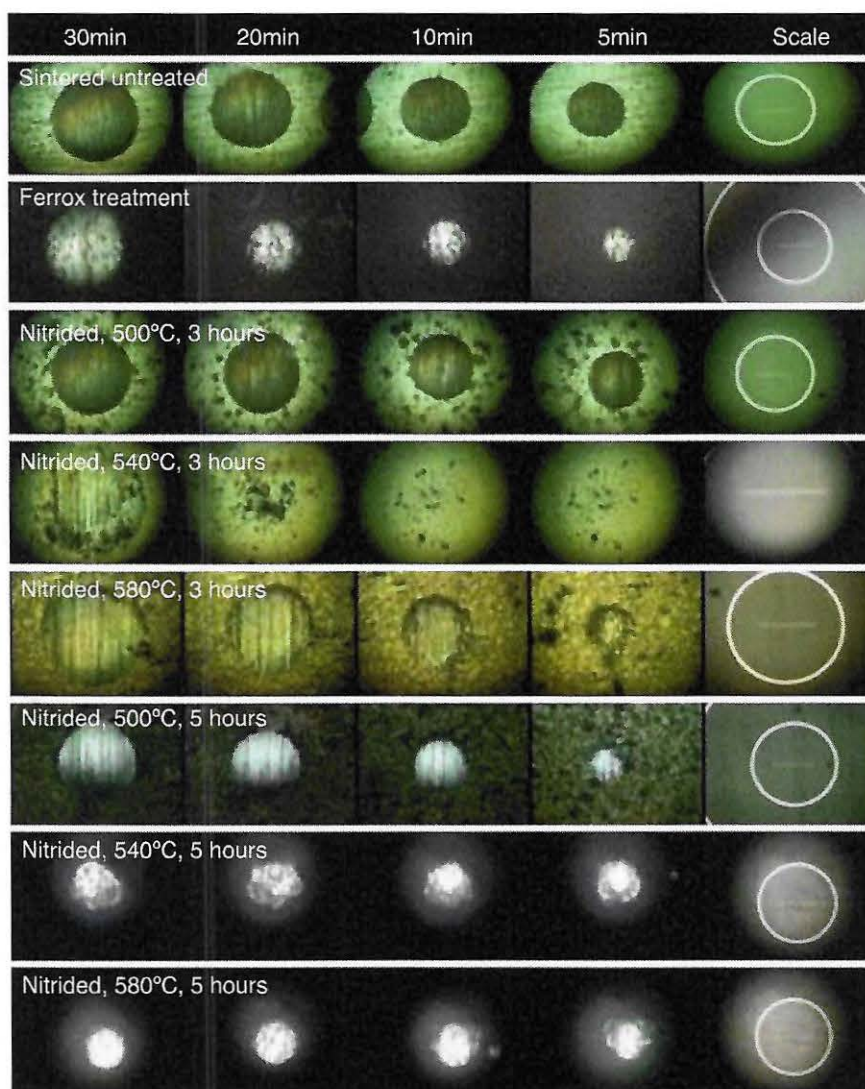


Fig. 8 – Images of the wear caps for different amplifications.

relatively thin nitrided layer, whose depth is significantly smaller than the probe depth of the XRD technique. The intensities of the  $\gamma'$ -Fe<sub>4</sub>N are greater at higher nitriding temperatures and 5 h of treatment.

### 3.3. Wear evaluation

Fig. 8 shows the images of the wear caps for all samples in different amplifications. The wear volumes (in mm<sup>3</sup>) as a function of testing times are plotted in Fig. 9.

It can be observed that the nitrided samples present better wear resistance than the untreated sample or the sample submitted to the ferrox treatment, regardless of the testing conditions. Lower wear rate values are obtained for the samples nitrided for 5 h at 540 and 580 °C, indicating that higher nitriding temperatures and times had a more favorable impact on the wear resistance.

The sample submitted to ferrox treatment presents good wear resistance, but the wear loss after 30 min of wear test is more pronounced than the wear loss values for the nitrided samples. This is probably due to the small thickness of the ferrox layer (about 3.5 μm), and the sudden increase in wear volume might be associated with the perforation of the ferrox layer, leading to the untreated substrate.

### 3.4. Microhardness evaluation

Fig. 10 depicts the Vickers microhardness test results for all samples. Higher values were obtained for the samples nitrided at 580 °C for 3 and 5 h, while lower values were obtained at a nitriding temperature of 500 °C. The hardness increased 83% for the sample nitrided at 580 °C for 5 h in comparison with that of the untreated sample, and it increased 31% in comparison with the hardness of the sample submitted to the ferrox

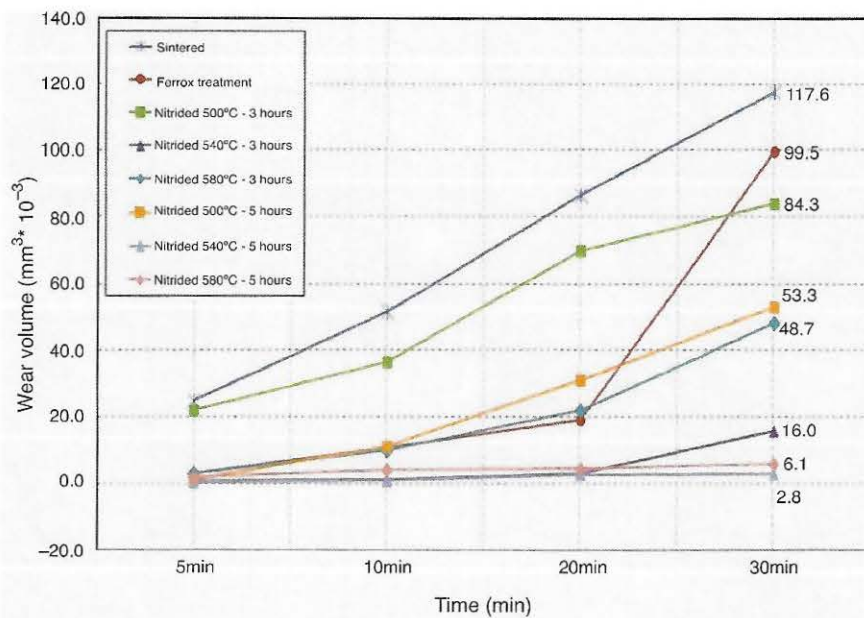


Fig. 9 – The wear volumes (in  $\text{mm}^3$ ) as a function of testing times.

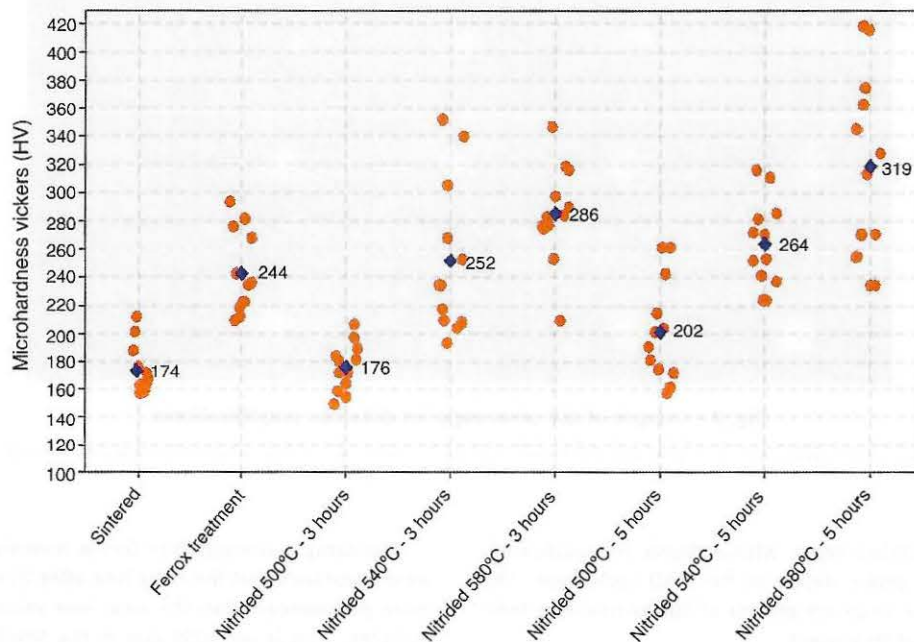


Fig. 10 – Vickers microhardness test results.

treatment. These findings demonstrate the effectiveness of the plasma nitriding treatment.

#### 4. Conclusions

Sintered ferrous alloy samples were plasma nitrided at 500, 540, and 580 °C for 3 and 5 h and then characterized by SEM and XRD. For comparison, a ferrox-treated ferrous alloy sample was also characterized. Regarding the thickness dependence,

the temperature variable predominates over the nitriding time variable. According to Fick's second law, the nitride layer thickness is less dependent on  $t$  – time (non-linearly) than on  $T$  – temperature (exponentially).

The nitrided layer consists predominantly of  $\gamma'$ -Fe<sub>4</sub>N phase, with a smaller amount of  $\epsilon$ -Fe<sub>3</sub>N phase. The amount of the  $\gamma'$ -Fe<sub>4</sub>N phase increases with higher nitriding temperatures and longer times.

Higher nitriding temperatures and times enhanced both the wear resistance and the hardness of the samples.



## Funding

Brazilian agencies CNPq (grant no. 302001/1010-7) and FAPESP.

## Conflicts of interest

The authors declare no conflicts of interest.

## REFERENCES

- [1] Fernandes FAP, Lombardi Neto A, Casteletti LC, Oliveira AM, Totten GE. Stainless steel property improvement by ion nitriding and nitrocarburizing. *Heat Treat Prog* 2008;8:41-3.
- [2] Michel H, Czerwicz T, Gantois M, Ablitzer D, Ricard A. Progress in the analysis of the mechanisms of ion nitriding. *Surf Coat Technol* 1995;72:103-11.
- [3] Cocke DL, Jurcikrajman M, Veprek S. The surface-properties and reactivities of plasma-nitrided iron and their relation to corrosion passivation. *J Electrochem Soc* 1989;136:3655-62.
- [4] Gontijo LC, Machado R, Miola EJ, Casteletti LC, Nascente PAP. Characterization of plasma-nitrided iron by XRD, SEM and XPS. *Surf Coat Technol* 2004;183:10-7.
- [5] Inokuti Y, Nishida N, Ohashi N. Formation of  $\text{Fe}_3\text{N}$ ,  $\text{Fe}_4\text{N}$  and  $\text{Fe}_{16}\text{N}_2$  on surface of iron. *Metall Trans A* 1975;6:773-84.
- [6] Reisse G, Ebersbach U, Henny F, Weissmantel C. Ion beam nitriding of iron. *Thin Solid Films* 1979;61:L9-11.
- [7] Metin E, Inal OT. Formation and growth of iron nitrides during ion-nitriding. *J Mater Sci* 1987;22:2783-8.
- [8] Xu SL, Wang L, Yu ZW, Hei ZK. Transmission electron microscopy study on the cross-sectional microstructure of an ion-nitriding layer. *Metall Trans A* 1996;27:1347-52.
- [9] Salas O, Figueroa U, Palacios M, Oseguera. Mechanisms of phase formation during post-discharge nitriding. *Surf Coat Technol* 1996;86-87:332-7.
- [10] Miola EJ, de Souza SD, Nascente PAP, Olzon-Dionysio M, Olivieri CA, Spinelli D. Studies on plasma-nitrided iron by scanning electron microscopy, glancing angle X-ray diffraction, and X-ray photoelectron spectroscopy. *J Vac Sci Technol A* 2000;18:2733-7.
- [11] Muñoz Riofano RM, Casteletti LC, Nascente PAP. Study of the wear behavior of ion nitrided steels with different vanadium contents. *Surf Coat Technol* 2006;200:6101-10.
- [12] Collins GA, Hutchings R, Short KT, Tendys J, Van Der Valk CH. Development of a plasma immersion ion implanter for the surface treatment of metal components. *Surf Coat Technol* 1996;84:537-43.
- [13] Borgioli F, Fossati A, Galvanetto E, Bacci T. Glow-discharge nitriding of AISI 316L austenitic stainless steel: influence of treatment temperature. *Surf Coat Technol* 2005;200:2474-80.
- [14] Borgioli F, Fossati A, Galvanetto E, Bacci T, Pradelli G. Glow discharge nitriding of AISI 316L austenitic stainless steel: influence of treatment pressure. *Surf Coat Technol* 2005;200:5505-13.
- [15] Fernandes FAP, Heck SC, Pereira RG, Picon CA, Nascente PAP, Casteletti LC. Ion nitriding of a superaustenitic stainless steel: wear and corrosion characterization. *Surf Coat Technol* 2010;204:3087-90.
- [16] Rutherford KL, Hutchings IM. A microabrasive wear test, with particular application to coated systems. *Surf Coat Technol* 1996;79:231-9.
- [17] Hoffmann FT, Mayr P. Nitriding and nitrocarburizing. *ASM Handb* 1992;18:878-83.

